Supplementary Information

Highly stable PEDOT coatings realized via a simple yet robust charge regulation strategy

Xiaojing Xu, [a] Yuting Diao, [a] Yanzhuo Zhu, [a] Jingyi Xiong, [a] Qi Guo, [a] Xiangyu Li [b] and Yuda Li *[a,c]

[a] *Key Laboratory of Green Chemical Engineering Process of Ministry of Education, School of Chemical Engineering and Pharmacy, Wuhan Institute of Technology, Wuhan, Hubei 430205, China.*

[b] *CABIO Biotechnology (Wuhan) Co., Ltd., Wuhan, Hubei 430223, China.*

[c] *Department of Chemical and Materials Engineering, University of Alberta, Edmonton, Alberta T6G 1H9, Canada*

*Corresponding author: E-mail: psydli@wit.edu.cn

1. Experimental Section

1.1 Materials

PSS with *Mw* of 200 KDa was procured from Sigma-Aldrich. FDN was obtained from Zhanjiang Admixture Factory. EDOT monomer was purchased from Sigma-Aldrich. APS, $FeCl_3$, H_2SO_4 (95–98 wt%), ethylenediamine, DIO, PE, n-Hex, Tol, n-BuOH, EA, CF, acetone, and ethanol were acquired from Sinopharm Chemical and used without further purification.

1.2 Synthesis of PEDOT CPs and thin-film preparation

In a typical protocol preparation, 40 mL of deionized water was charged with PSS powder under continuous stirring, followed by the addition of EDOT monomer under slow stirring conditions for 60 min. Controlled acidification to pH 1.2 preceded the dropwise addition of APS solution, with stirring immediately increased to 800 rpm to achieve optimal oxidant dispersion. The mass ratio of EDOT to PSS is 1:2 and the mole ratio of APS to $FeCl_3$ to EDOT is 1.5:0.05:1. The reaction mixture was maintained

under continuous stirring at room temperature for 24 h, and dialyzed using a membrane with a 1000 cutoff for 5 days. Ultimately, the PEDOT aqueous dispersion was concentrated to a mass concentration of 1.3% via the process of rotary evaporation. The preparation method for PEDOT:FDN was identical.

The thin films were prepared through the following procedure: (1) Glass substrates were mounted on a glass holder and sequentially ultrasonicated in detergent-containing deionized water, pure deionized water, acetone, and ethanol (20 min each), followed by nitrogen drying; (2) Prior to use, the substrates were treated with UV/ozone for 25 min; (3) Thin films were prepared by spin-coating 35 μL aliquots of the CPs solution onto the pre-treated substrates at 2000 rpm for 60 s, yielding optically transparent and homogeneous PEDOT films; (4) The films were finally annealed at 120°C for 15 min on a hot plate to obtain PEDOT:PSS and PEDOT:FDN thin films.

1.3 Reagents post-treatment of CPs thin films

1.3.1 Organic reagents post-treatment process

DIO post-treatment process: PEDOT CPs thin films were placed in glass dishes with 100 μL of DIO uniformly distributed nearby. The dishes were covered and incubated at 50°C for 5 min to allow vapor-phase treatment. Subsequently, the films were transferred to a spin-coater and rotated at 2000 rpm for 1 min to remove excess solvent.

PE post-treatment process: The films were immersed in glass dishes containing 6 mL of PE solution, covered, and allowed to stand for 5 min. After treatment, the films were spin-coated at 2000 rpm for 1 min to ensure uniform solvent removal.

Identical procedures were applied using n-Hex, Tol, n-BuOH, EA, and CF as processing solvents, following the PE post-treatment process.

1.3.2 H_2SO_4 post-treatment process

The films were first immersed in 98% H_2SO_4 and thoroughly rinsed three times with deionized water, followed by annealing at the optimized temperature. The same H_2SO_4 immersion and rinsing procedure was then repeated, after which a final annealing step at the same temperature completed the post-treatment process.

1.4 Temporal Evolution of Sheet Resistance in PEDOT-Based Films

For untreated PEDOT CPs films, the initial sheet resistance (R_0) was measured

immediately after fabrication (following Section 1.2 protocols) using a standard four point probe system. The characterized films were stored in desiccators under atmospheric conditions of 25°C and 60% relative humidity between measurements. Subsequent sheet resistance (R) values were recorded at designated time intervals using identical measurement conditions.

Films subjected to H_2SO_4 immersion treatment (prepared per Section 1.3.2) underwent identical resistance monitoring procedures. This standardized protocol enabled systematic tracking of temporal resistance evolution under ambient storage conditions.

1.5 Measurements and characterizations

Elemental analysis (EA) was performed using an Elementar UNICUBE analyzer in CHNS mode. DLS measurements were performed using a Malvern Nano-ZS90 particle size/Zeta potential analyzer. UV-vis-NIR absorption spectra were acquired with a Shimadzu UV-3100 spectrophotometer. Optical microscopy imaging was carried out using an MF23 instrument (Guangzhou Micro-shot Technology). XPS measurements were obtained with a Thermo Scientific ESCALAB 250Xi spectrometer. The S 2p peaks appeared at approximately 162 eV and 160 eV were deconvoluted into two doublets: oxidized sulfur in PEDOT at medium binding energies (~162.9 eV and ~162.0 eV), and neutral sulfur in PEDOT at lower binding energies (~161.5 eV and ~160.6 eV). By calculating the relative intensities of the two PEDOT sulfur components, the doping level was determined.[1] AFM characterizations were performed in tapping mode using a Park XE-100 system. The σ characterizations were determined via four point probe measurements, while film thickness tests were quantified with a Dektak150 profilometer. Static contact angles were measured using a JC2000C1 goniometer.

1.6 In-Plane Conductivity Characterizations of PEDOT CPs Thin Films

The in-plane conductivity ($\sigma_{//}$) was characterized on a Glass/PEDOT/Ag cell following previously reported procedures.[2] The $\sigma_{//}$ was calculated according to the relationship $\sigma_{//} = L/(a \cdot d \cdot R_l)$, where L represents the inter-electrode distance, a denotes the electrode length, d is the film thickness, and R_l corresponds to the resistance at channel length L ($R_l = \Delta R/\Delta n$). The linear dependence of resistance on progressively increased Ag electrode spacing was systematically characterized to ensure measurement accuracy.

2. Supplementary figures and tables

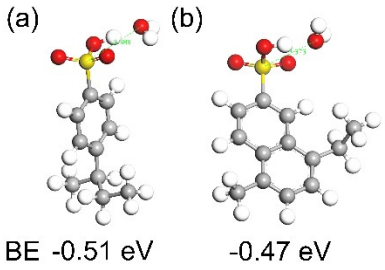

Fig. S1 MD simulations showing (a) the binding energy between water molecules and the PSS structural unit, and (b) that between water molecules and the FDN structural unit.

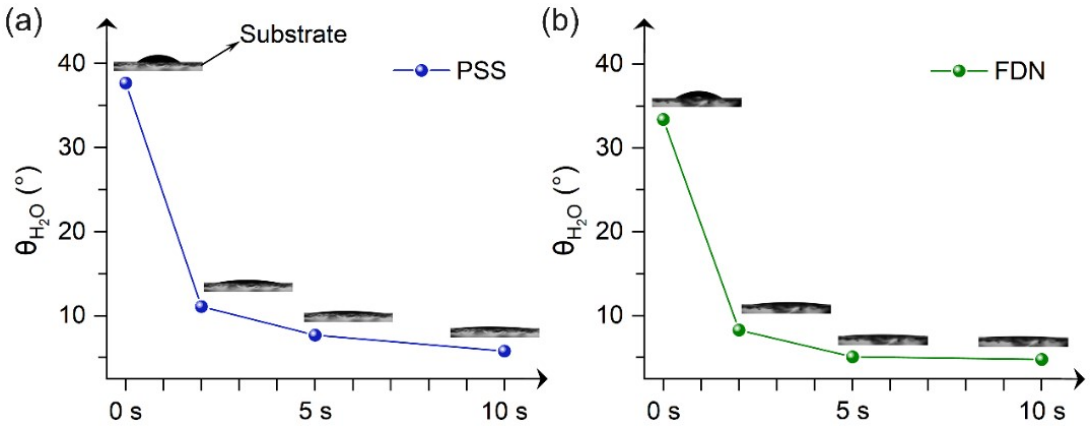

Fig. S2 Temporal evolution of water droplet contact angles on PSS and FDN films. The nearly identical initial contact angles and spreading behaviors indicate comparable hydrophilicity between the two polyanions.

Table S1 The mass contents of elements (N, C, H, S) and the sulfonic acid group contents in PSS and FDN.

Sample	Element content (wt%)				Sulfonic group (mmol/g)
	N	C	H	S	
PSS	0.178	40.941	4.585	13.676	4.274
FDN	0.238	49.469	4.492	10.823	3.382

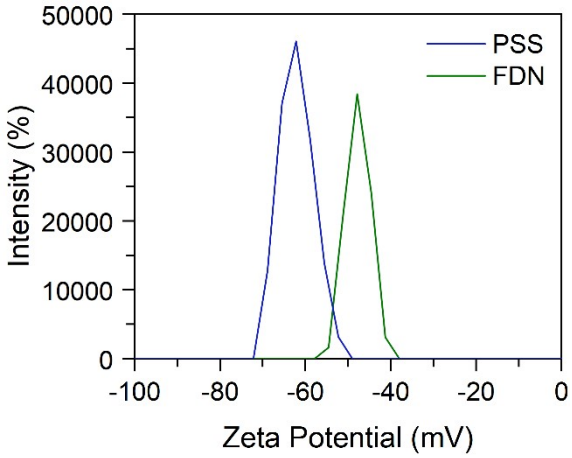

Fig. S3 ζ potential profiles of PSS and FDN.

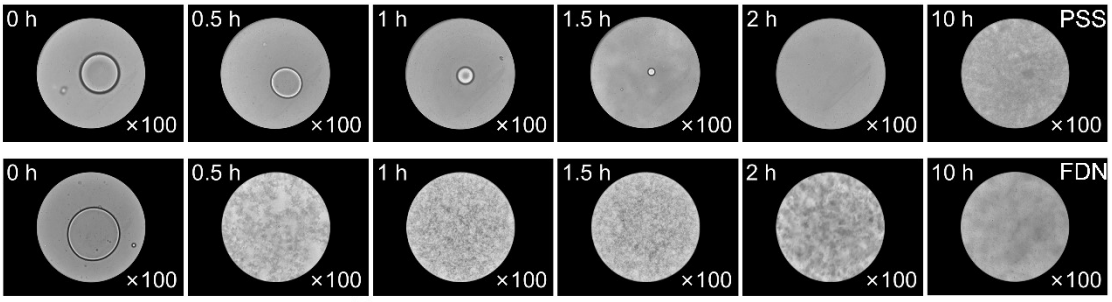

Fig. S4 Microscopic images of EDOT droplets within PSS and FDN system at different time intervals.

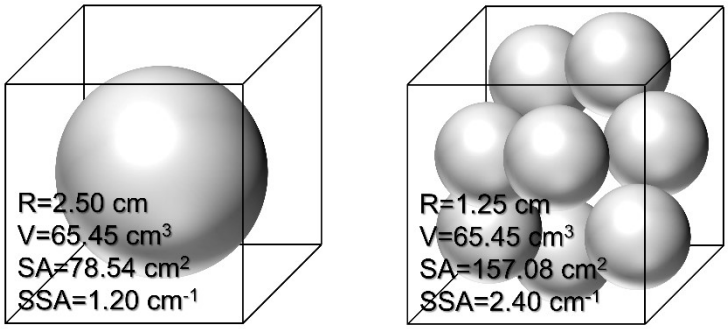

Fig. S5 Schematic illustration of the variations in surface area (SA) and specific surface area (SSA) among spheres of different sizes but identical volumes.

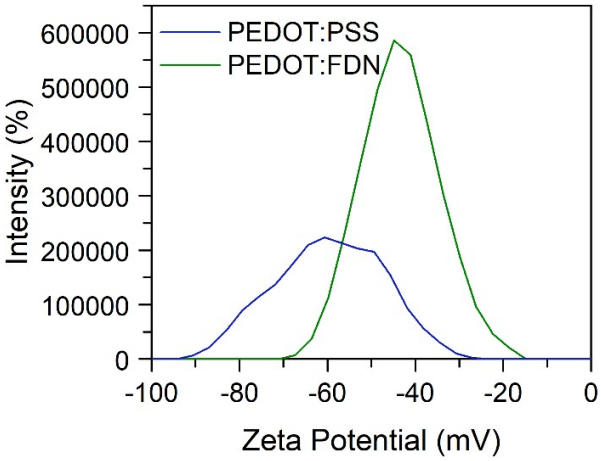

Fig. S6 ζ potentia profiles of PEDOT:PSS and PEDOT:FDN aqueous solutions.

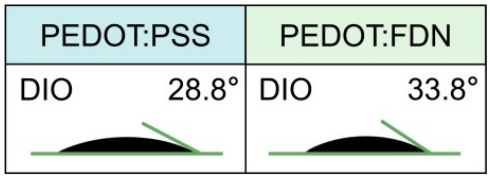

Fig. S7 Contact angles of DIO droplets on PEDOT:PSS and PEDOT:FDN films.

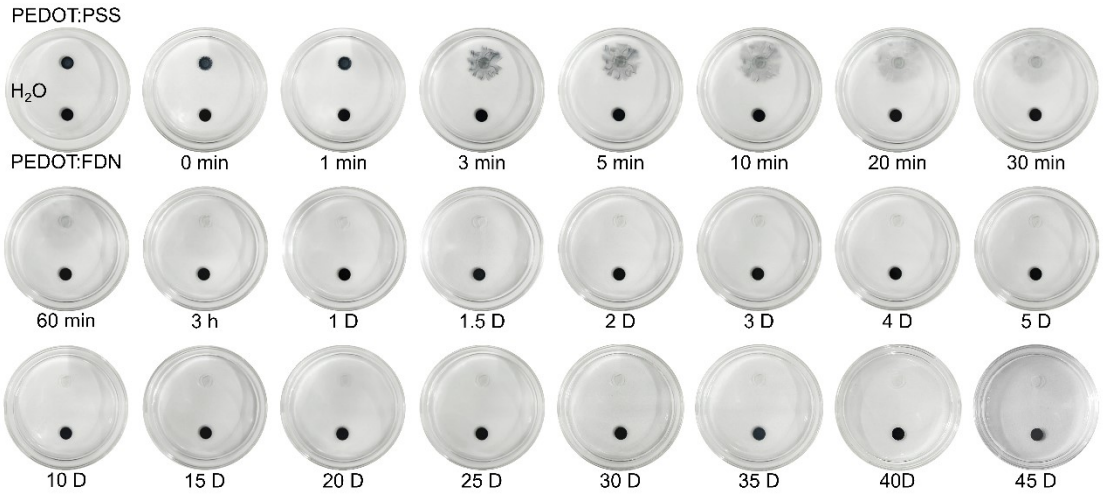

Fig. S8 Digital photos of Glass/PEDOT:PSS (Top) and Glass/FDN (down) immersed in water as a function of immersion duration.

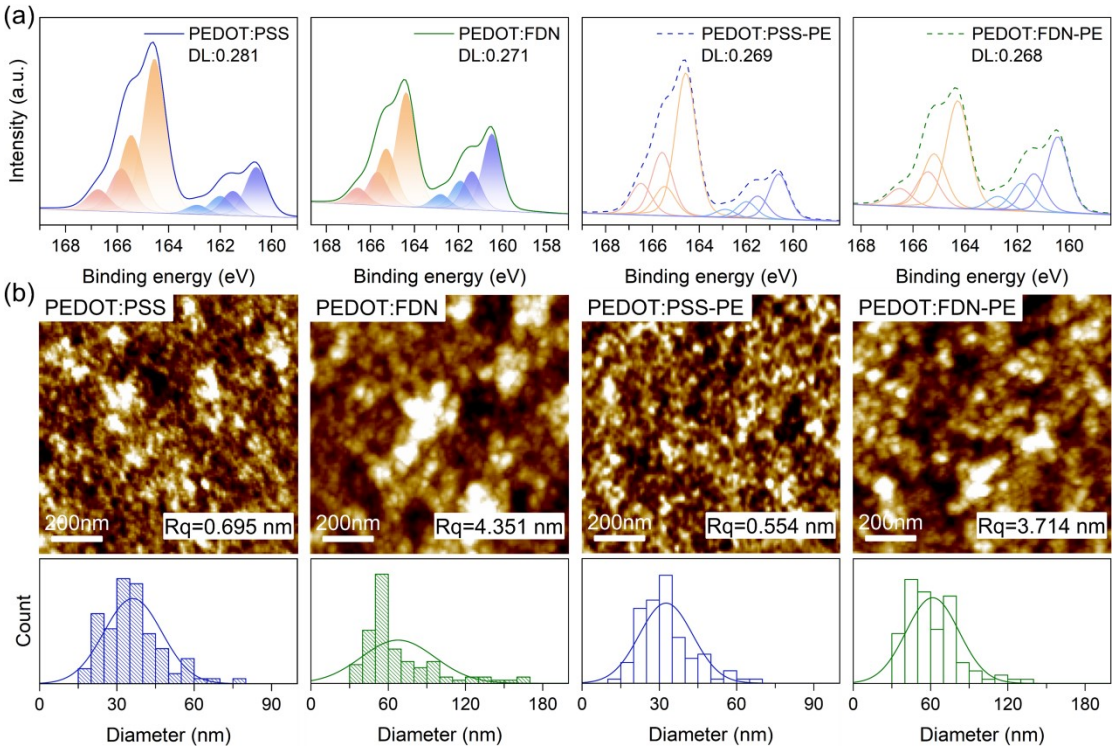

Fig. S9 Structural features of PEDOT:PSS and PEDOT:FDN. (a) XPS spectra of PEDOT:PSS and PEDOT:FDN films before and after PE treatment; (b) AFM height images and size distribution diagrams of PEDOT:PSS and PEDOT:FDN films before and after PE treatment.

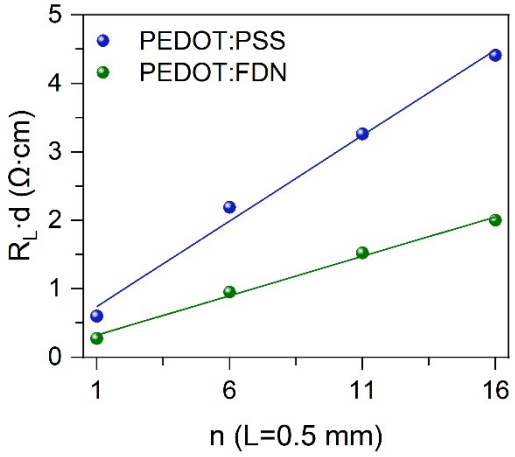

Fig. S10 Measured resistance of PEDOT:PSS and PEDOT:FDN films as a function of channel length

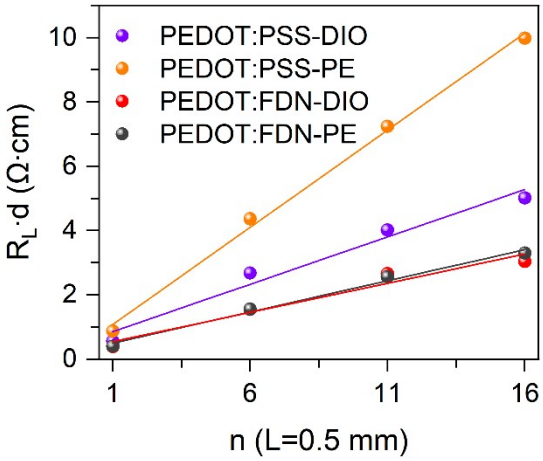

Fig. S11 Measured resistance of PEDOT:PSS-DIO, PEDOT:PSS-PE, PEDOT:FDN-DIO and PEDOT:FDN-PE films as a function of channel length

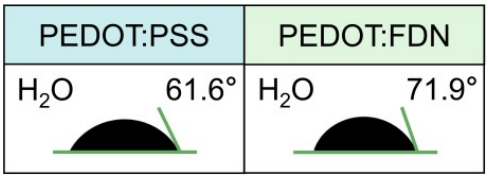

Fig. S12 Contact angles of water droplets on PEDOT:PSS and PEDOT:FDN films.

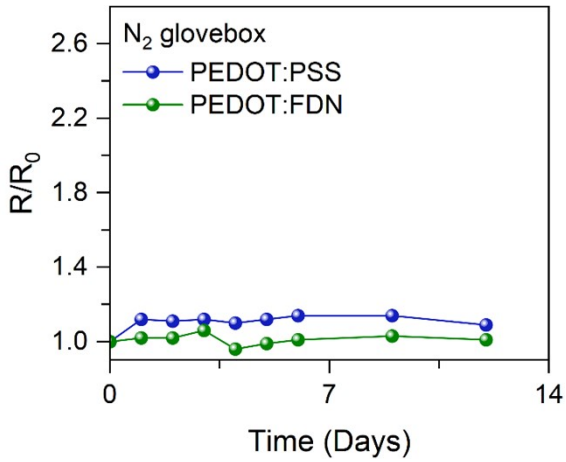

Fig. S13 Evolution of the electrical resistance of PEDOT:PSS and PEDOT:FDN films stored in a nitrogen atmosphere over time.

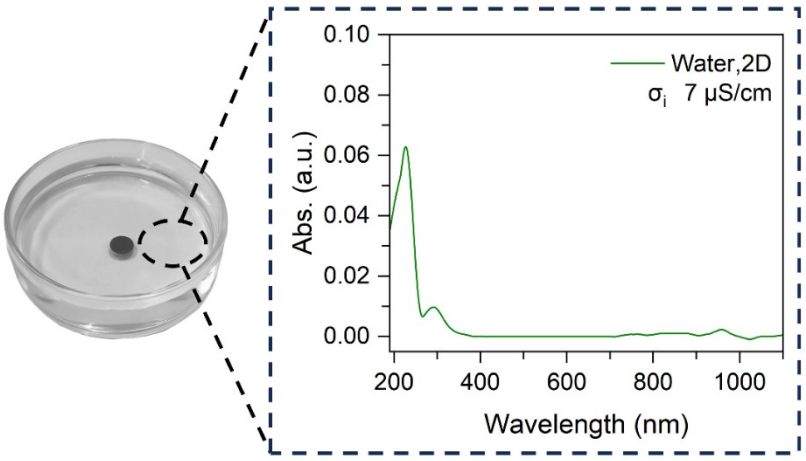

Fig. S14 Digital photographs of Glass/PEDOT:FDN immersed in deionized water, along with the measured UV-vis-NIR spectrum and ionic conductivity of the aqueous solution after two days of immersion. The ionic conductivity of deionized water was measured to be 5 uS/cm. The detection of FDN characteristic absorption, along with the observed increase in ionic conductivity, confirms the dissolution of surface-free FDN from the PEDOT:FDN film.

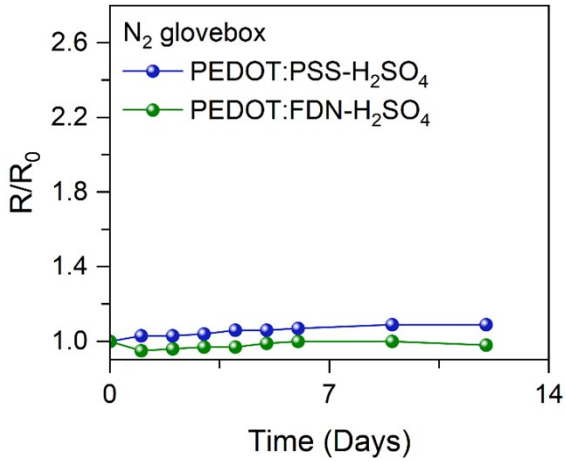

Fig. S15 Evolution of the electrical resistance of H_2SO_4 post-treated PEDOT:PSS and PEDOT:FDN films stored in a nitrogen atmosphere over time.

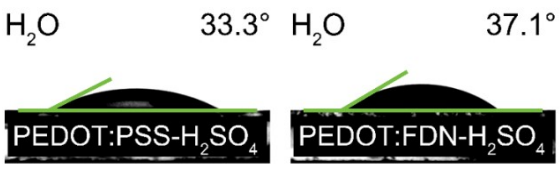

Fig. S16 Contact angles of water droplets on H_2SO_4 post-treated PEDOT:PSS and PEDOT:FDN films.

Fig. S17 Schematic illustration of the H_2SO_4 post-treatment mechanism.

References

1. Y. Song, J. Tang, Y. Qi, J. Zhang, Y. Li and F. Wang, *Polymer*, 2023, **266**, 125649.
2. Y. Jiang, X. Dong, L. Sun, T. Liu, F. Qin, C. Xie, P. Jiang, L. Hu, X. Lu, X. Zhou, W. Meng, N. Li, C. J. Brabec and Y. Zhou, *Nat. Energy*, 2022, **7**, 352-359.